Delft University of Technology

Delft Center for Systems and Control

Technical report 12-006

Integrated macroscopic traffic flow, emission, and fuel consumption model for control purposes*

S.K. Zegeye, B. De Schutter, J. Hellendoorn, E.A. Breunesse, and A. Hegyi

If you want to cite this report, please use the following reference instead:
S.K. Zegeye, B. De Schutter, J. Hellendoorn, E.A. Breunesse, and A. Hegyi, "Integrated macroscopic traffic flow, emission, and fuel consumption model for control purposes," *Transportation Research Part C*, vol. 31, pp. 158–171, June 2013.

Delft Center for Systems and Control
Delft University of Technology
Mekelweg 2, 2628 CD Delft
The Netherlands
phone: +31-15-278.24.73 (secretary)
URL: `https://www.dcsc.tudelft.nl`

*This report can also be downloaded via `https://pub.deschutter.info/abs/12_006.html`

Integrated Macroscopic Traffic Flow, Emission, and Fuel Consumption Model for Control Purposes

S. K. Zegeye[a,*], B. De Schutter[a], J. Hellendoorn[a], E. A. Breunesse[b], A. Hegyi[c]

[a] *Department of Delft Center for Systems and Control, Delft University of Technology, Mekelweg 2, 2628 CD, Delft, The Netherlands*
[b] *Shell Nederland B.V., Carel van Bylandtlaan 30, 2596 HR, The Hague, The Netherlands*
[c] *Department of Transport & Planning, Delft University of Technology, Stevinweg 1, 2628 CN, Delft, The Netherlands.*

Abstract

Traffic control approaches based on on-line optimization require fast and accurate integrated models for traffic flow, emission, and fuel consumption. In this context, one may want to integrate macroscopic traffic flow models with microscopic emission and fuel consumption models, which can result in shorter simulation times with fairly accurate estimates of the emissions and fuel consumption. In general, however, macroscopic traffic flow models and microscopic emission and fuel consumption models cannot be integrated with each other. We provide a general framework to integrate these two kinds of models. We illustrate the approach by considering the macroscopic traffic flow model METANET[1] and the microscopic emission and fuel consumption model VT-micro[2], resulting in the so called the "VT-macro" model. Moreover, we characterize analytically the error introduced by the VT-macro model relative to the original VT-micro model. We further present an empirical analysis of the error and the computation time based on calibrated models of the Dutch A12 freeway.

1. Introduction

One of the reasons that makes traffic control a challenging discipline is the nature of the system. Traffic systems are very complex, nonlinear, and are affected by many external and internal factors. In addition to the vehicle dynamics with respect to the infrastructure, the human driver is the main element of traffic systems. This augments the complexity and stochasticity of the systems. It is, therefore, challenging to capture all the traffic phenomena with a

*Corresponding author
Email addresses: s.k.zegeye@tudelft.nl (S. K. Zegeye), b.deschutter@tudelft.nl (B. De Schutter), j.hellendoorn@tudelft.nl (J. Hellendoorn), ewald.breunesse@shell.com (E. A. Breunesse), a.hegyi@tudelft.nl (A. Hegyi)

[1] METANET (Messmer and Papageorgiou, 1990) stands for "Modèle d'Ecoulement du Trafic Autoroutier: NETwork".

[2] VT-micro (Ahn et al., 1999) stands for "Virginia Tech Microscopic"

single model of the system. Based on the intended application, a variety of approaches can be used to model traffic systems (Hoogendoorn and Bovy, 2001). Some models consider the dynamics of individual vehicles (or the response of individual drivers) (Brackstone and McDonald, 2000; Gazis et al., 1961; Pipes, 1953). Such traffic models are classified as microscopic traffic flow models. Other models are based on the average behavior of the traffic flow without describing the dynamics of individual vehicles in the traffic network; and are called macroscopic traffic flow models (Chen et al., 2004; Daganzo, 1994, 1995; Messmer and Papageorgiou, 1990). There are also developments that combine some of the characteristics of macroscopic models and some characteristics of microscopic models (Hoogendoorn and Bovy, 2000). In general, the main difference between the models is the trade-off between optimizing simulation speeds and estimating the traffic states (or traffic phenomena) as accurately as possible. As a result there is a large variety of traffic flow models. A detailed literature survey on traffic flow models can be found in (Hoogendoorn and Bovy, 2001). In the sequel we will present a short introduction to traffic emission and fuel consumption models and the way they are used with traffic flow models.

Traffic emission and fuel consumption models provide the estimate or prediction of emission and fuel consumption of vehicles in a traffic flow based on the operating conditions of the vehicles. Similar to traffic flow models, traffic emission and fuel consumption models also differ based on the modeling approaches used. Just like traffic flow models, emission and fuel consumption models can be either macroscopic (such as average-speed-based models) (Chang and Herman, 1981; Evans and Herman, 1978; Ntziachristos and Samaras, 2000) or microscopic (also called dynamic models) (Ahn et al., 1999; An et al., 1997). Average-speed-based models estimate the emission and fuel consumption of a traffic flow based on the trip-based average speed (Evans and Herman, 1978; Boulter et al., 2002; Ntziachristos and Samaras, 2000). On the other hand, dynamic emission or fuel consumption models estimate the emission or fuel consumption based on the instantaneous traffic variables of individual vehicles (Boulter et al., 2002; Ahn et al., 1999; Ahn and Rakha, 2008). Average-speed-based models are more coarse than dynamic emission models, and compared to the dynamic emission models they are simpler to use and allow to compute faster the estimates of emissions. However, average-speed-based models do not capture the emissions or fuel consumption due to the variation of the speed of the traffic (Ahn and Rakha, 2008; Boulter et al., 2002). Since the input for microscopic emission and fuel consumption models is the operating condition of individual vehicles the computation time required is proportional to the number of vehicles. But the input for macroscopic emission and fuel consumption models is the average operating condition of a group of vehicles. Hence, the computation time of the macroscopic models is reduced as compared to the microscopic models.

Macroscopic emission and fuel consumption models are in principle used with macroscopic traffic flow models, and the microscopic emission and fuel consumption models are used with microscopic traffic flow models. For example in (Rakha and Ahn, 2004), an integrated microscopic traffic flow model and emission model has been used for quantifying the environmental impacts of ITS

alternatives. Moreover, a study in (Huang and Ma, 2009) shows the integration of a microscopic emission and fuel consumption model with a microscopic traffic flow model using a distributed framework to tackle computation time. In both (Rakha and Ahn, 2004) and (Huang and Ma, 2009) the integration is based on microscopic traffic flow and microscopic emission and fuel consumption models. In general, the output of the macroscopic traffic flow models can be easily fed to macroscopic emission and fuel consumption models and the output of microscopic traffic flow models can be easily fed to microscopic emission and fuel consumption models. This means that the choice we make on the traffic flow models also affects our choice on the emission and fuel consumption models. Hence, the accuracy of the estimates of the emission and fuel consumed cannot be enhanced if one uses macroscopic models unless the macroscopic emission and fuel consumption models are themselves accurate. But as studies show the available macroscopic emission and fuel consumption models do not provide accurate estimations relative to microscopic emission and fuel consumption models (Ahn and Rakha, 2008; Boulter et al., 2002).

So, to get a balanced trade-off between computational complexity and accuracy, one may want to combine macroscopic traffic flow modes with microscopic emission and fuel consumption models. However, this is not straightforward. The macroscopic outputs of the macroscopic traffic models should be transformed into microscopic variables. Moreover, the error that can be introduced due to such approximations is not known. Therefore, in this paper we present an approach to integrate these two types of models so that the macroscopic variables can be used to produce relatively accurate estimates of the emissions and the fuel consumption. We also show the improvement in the simulation time as compared to the microscopic models.

We illustrate the integration approach by considering the macroscopic traffic flow model METANET (Messmer and Papageorgiou, 1990) and the microscopic emission and fuel consumption model VT-micro (Ahn et al., 1999). The integration results in an integrated macroscopic traffic flow, emission, and fuel consumption model. We designate the new macroscopic-variable-based dynamic emission and fuel consumption model as the VT-macro model. We provide an analytic solution to the maximum error that can be introduced due to the approximation in the transformation of the macroscopic variables into microscopic ones. Moreover, the error is further empirically assessed using models calibrated to part of the Dutch A12 freeway for different demand scenarios. We have also conducted computation time comparisons for these different demand scenarios.

The remainder of the paper is organized as follows. The traffic flow model and emission and fuel consumption model used are discussed in Section 2. Section 3 elaborates the integration of macroscopic traffic flow models with microscopic emission and fuel consumption models. In Section 4 and Section 5, we provide and discuss the relative error of the newly developed macroscopic emission and fuel consumption model analytically and empirically respectively. Finally, the paper is concluded in Section 6.

2. Models

Although the integration approach to be presented in Section 3 is generic (i.e. the approach can also be applied to other macroscopic traffic flow models and microscopic emission and fuel consumption models), we present it by considering two specific models: METANET (Messmer and Papageorgiou, 1990) from the class of macroscopic traffic flow models and VT-micro (Ahn et al., 1999) from the class of microscopic emission and fuel consumption models. In this section we therefore briefly present METANET and VT-micro.

2.1. METANET

METANET (Messmer and Papageorgiou, 1990) is a macroscopic second-order traffic flow model. The model describes the evolution of the traffic variables — average density ρ [veh/km/lane], average flow q [veh/h], and average space-mean speed v [km/h] — as nonlinear difference equations. The METANET model is both temporally and spatially discretized. In the model, a node is placed wherever there is a change in the geometry of a freeway (such as a lane drop, on-ramp, off-ramp, or a bifurcation). A homogeneous freeway stretch that connects such nodes is called a link. Links are further divided into equal segments of length 300-500 m (Messmer and Papageorgiou, 1990). The equations that describe the traffic dynamics in a segment i of a link m are given by

$$q_{m,i}(k) = \lambda_m \rho_{m,i}(k) v_{m,i}(k) \tag{1}$$

$$\rho_{m,i}(k+1) = \rho_{m,i}(k) + \frac{T_\mathrm{s}}{L_m \lambda_m} \left[q_{m,i-1}(k) - q_{m,i}(k) \right] \tag{2}$$

$$\begin{aligned} v_{m,i}(k+1) = v_{m,i}(k) &+ \frac{T_\mathrm{s}}{\tau} [V[\rho_{m,i}(k)] - v_{m,i}(k)] \\ &+ \frac{T_\mathrm{s} v_{m,i}(k) \left[v_{m,i-1}(k) - v_{m,i}(k) \right]}{L_m} \\ &- \frac{T_\mathrm{s} \eta \left[\rho_{m,i+1}(k) - \rho_{m,i}(k) \right]}{\tau L_m \left(\rho_{m,i}(k) + \kappa \right)} \end{aligned} \tag{3}$$

$$V[\rho_{m,i}(k)] = v_{\mathrm{free},m} \exp \left[-\frac{1}{b_m} \left(\frac{\rho_{m,i}(k)}{\rho_{\mathrm{cr},m}} \right)^{b_m} \right] \tag{4}$$

where $q_{m,i}(k)$ denotes the outflow of segment i of link m during the time period $[kT_\mathrm{s}, (k+1)T_\mathrm{s}]$, $\rho_{m,i}(k)$ and $v_{m,i}(k)$, denote respectively the density and space-mean speed of segment i of link m at simulation time step k, L_m denotes the length of the segments of link m, λ_m denotes the number of lanes of link m, and T_s denotes the simulation time step (a typical value for T_s is 10 s). Furthermore, $\rho_{\mathrm{cr},m}$ is the critical density, τ a time constant, η the anticipation constant, b_m the parameter[3] of the fundamental diagram, and κ is a model parameter.

[3] In the original METANET model the parameter b_m is denoted by a_m. However, in order to avoid confusion with the acceleration (which will be indicated with a_m in this paper) we chose to use b_m.

For origins (such as on-ramps and mainstream entry points) a queue model is used. The dynamics of the queue length w_o at the origin o are modeled as

$$w_o(k+1) = w_o(k) + T_{\mathrm{s}}(d_o(k) - q_o(k)) \tag{5}$$

where $d_o(k)$ and $q_o(k)$ denote respectively the demand and outflow of the origin o at simulation time step k with

$$q_o(k) = \min\left[d_o(k) + \frac{w_o(k)}{T_{\mathrm{s}}},\ C_o,\ C_o\left(\frac{\rho_{\mathrm{jam},m} - \rho_{m,1}(k)}{\rho_{\mathrm{jam},m} - \rho_{\mathrm{cr},m}}\right)\right], \tag{6}$$

for a mainstream origin or an unmetered on-ramp, and

$$q_o(k) = \min\left[d_o(k) + \frac{w_o(k)}{T_{\mathrm{s}}},\ r_o(k)C_o,\ C_o\left(\frac{\rho_{\mathrm{jam},m} - \rho_{m,1}(k)}{\rho_{\mathrm{jam},m} - \rho_{\mathrm{cr},m}}\right)\right] \tag{7}$$

for a metered on-ramp, where m is the index of the link to which the main-stream origin or on-ramp is connected, $\rho_{\mathrm{jam},m}$ and $\rho_{\mathrm{cr},m}$ are respectively the maximum and critical densities of link m, $r_o(k) \in [0,1]$ denotes the ramp metering rate for on-ramp o for simulation step k, and C_o denotes the capacity of on-ramp or mainstream origin o.

If m is the link out of a node to which an on-ramp o is connected, then for the first segment of link m the term

$$-\frac{\delta T_{\mathrm{s}} q_o(k) v_{m,1}(k)}{L_m \lambda_m (\rho_{m,1}(k) + \kappa)} \tag{8}$$

is added to (3) in order to account for the speed drop caused by the merging phenomena, where δ is model parameter.

In case the number of lanes changes, a node n is placed. Let m and $m+1$ be the indices of respectively the ingoing and outgoing links of node n. Then, the space-mean speed of the last segment N_m of link m is either reduced or increased by adding the weaving phenomena term

$$-\frac{\phi T_{\mathrm{s}} \Delta\lambda_m \rho_{m,N_m}(k) v^2_{m,N_m}(k)}{L_m \lambda_m \rho_{\mathrm{cr},m}} \tag{9}$$

where ϕ is a model parameter and $\Delta\lambda_m = \lambda_m - \lambda_{m+1}$ denotes the number of lanes dropped or increased.

A node provides a (virtual) downstream density to incoming links, and a (virtual) upstream speed to leaving links. The flow that enters node n is distributed among the leaving links according to

$$Q_n(k) = \sum_{\mu \in \mathcal{I}_n} q_{\mu,N_\mu}(k) \tag{10}$$

$$q_{m,0}(k) = \beta_{n,m}(k) Q_n(k) \tag{11}$$

where $Q_n(k)$ is the total flow that enters the node at simulation step k, $\mathcal{I}_n$ is the set of links that enter node n, $\beta_{n,m}(k)$ are the turning rates (i.e., the fraction

of the total flow through node n that leaves via link m), and $q_{m,0}(k)$ is the flow that leaves node n via link m.

When node n has more than one leaving link, the virtual downstream density $\rho_{m,N_m+1}(k)$ of entering link m is given by

$$\rho_{m,N_m+1}(k) = \frac{\sum_{\mu\in\mathcal{O}_n} \rho_{\mu,1}^2(k)}{\sum_{\mu\in\mathcal{O}_n} \rho_{\mu,1}(k)} \tag{12}$$

where $\mathcal{O}_n$ is the set of links leaving node n.

When node n has more than one entering link, the virtual upstream speed $v_{m,0}(k)$ of leaving link m is given by

$$v_{m,0}(k) = \frac{\sum_{\mu\in\mathcal{I}_n} v_{\mu,N_\mu}(k) q_{\mu,N_\mu}(k)}{\sum_{\mu\in\mathcal{I}_n} q_{\mu,N_\mu}(k)}. \tag{13}$$

2.2. VT-micro

VT-micro (Ahn et al., 1999) is a microscopic dynamic emission and fuel consumption model that yields the emission and fuel consumption rate of an individual vehicle α using the second-by-second speed and acceleration of the vehicle. We introduce a separate microscopic simulation time step T_m such that $T_\mathrm{m} \ll T_\mathrm{s}$ (typical value of $T_\mathrm{m} = 1\,\mathrm{s}$). Hence, we also define the microscopic simulation step counter ℓ. Consider a vehicle indexed by α. Now, the VT-micro model is mathematically expressed in the form

$$J_{\alpha,y}(\ell) = \exp\left(\tilde{v}_\alpha^\top(\ell) P_y \tilde{a}_\alpha(\ell)\right) \tag{14}$$

where $J_{\alpha,y}(\ell)$ is the estimate or prediction of the variable $y \in \{$CO emission, NO_x emission, HC emission, fuel consumption$\}$ at every microscopic simulation time step ℓ, the operator $\tilde{\cdot}$ defines the vectors of the speed v_α and the acceleration a_α as $\tilde{v}_\alpha(\ell) = [1\ v_\alpha(\ell)\ v_\alpha(\ell)^2\ v_\alpha(\ell)^3]^\top$ and $\tilde{a}_\alpha(\ell) = [1\ a_\alpha(\ell)\ a_\alpha(\ell)^2\ a_\alpha(\ell)^3]^\top$ for time step ℓ, and P_y denotes the model parameter matrix for the variable y. The values of the entries of P_y are given in Appendix A. Moreover, the emission and fuel consumption rates are respectively given in kg/s and l/s for the speed v_α in m/s and the acceleration a_α in $\mathrm{m/s^2}$.

The VT-micro emission model does not yield estimates of the CO_2 emission rate. However, in (Oliver-Hoyo and Pinto, 2008) it is shown that there is almost an affine relationship between fuel consumption and CO_2 emission. Then the CO_2 emission can be computed using the relation

$$J_{\alpha,\mathrm{CO_2}}(\ell) = \delta_1 v_\alpha(\ell) + \delta_2 J_{\alpha,\mathrm{fuel}}(\ell) \tag{15}$$

where $J_{\alpha,\mathrm{CO_2}}(\ell)$ denotes the CO_2 [kg/s] emission rate of vehicle α for time step ℓ, $J_{\alpha,\mathrm{fuel}}(\ell)$ denotes the fuel consumption rate in l/s for time step ℓ, with the model parameters $(\delta_1, \delta_2) = (1.17 \cdot 10^{-6}\,\mathrm{kg/m}, 2.65\,\mathrm{kg/l})$ for a diesel car and $(\delta_1, \delta_2) = (3.5 \cdot 10^{-8}\,\mathrm{kg/m}, 2.39\,\mathrm{kg/l})$ for a gasoline car.

3. Integration of the Models

In the sequel we present a general approach to integrate macroscopic traffic flow models with microscopic emission and fuel consumption models. This approach is generic and it can be adopted to most combinations of a macroscopic traffic flow model and a microscopic emission and fuel consumption model such as POLY (Qi et al., 2004), CMEM (Barth et al., 2000), and the microscopic models in (Joumard et al., 1995; Panis et al., 2006).

In order to integrate macroscopic traffic flow models with microscopic emission and fuel consumption models, we need to generate the average acceleration, average speed, and the number of vehicles subject to these variables at each simulation time step from the macroscopic traffic variables. This idea is illustrated in Fig. A.1. The macroscopic traffic variables (the average density, average space-mean speed, and average flow) are fed to the interface block. The interface block transforms these variables into variables that describe the average behavior of individual vehicles, i.e. it produces average speed, average acceleration, and the number of vehicles that are subject to the average speed and average acceleration.[4] Note that the macroscopic speed does not contain enough information to fully reconstruct the individual vehicle trajectories that would be needed to exactly calculate the microscopic emissions and fuel consumptions. The error that can be introduced by considering the average speed over a group of vehicles will be analyzed in Section 4.

Now we will illustrate the general integration approach using the METANET traffic flow model and VT-micro emission and fuel consumption model, which will result in a new dynamic macroscopic emission and fuel consumption model VT-macro, specifically derived for the METANET traffic flow model.

Since the METANET model is discrete both in space and in time there are two acceleration components involved in the model. The first is the "temporal" acceleration of the vehicles moving within a given segment. The second component is the "spatial-temporal" acceleration of the vehicles going from one segment to another from time step k to time step $k + 1$ (see Fig. A.2). The temporal and spatial-temporal accelerations describe the average dynamics of a group of vehicles. We will therefore also determine the number of vehicles that are subject to the corresponding accelerations. Hence, we generate triples of the form (a, v, n), where a represents the acceleration, v the speed, and n the number of vehicles involved.

3.1. Temporal Acceleration

By temporal acceleration we mean the acceleration of vehicles due to the change in space-mean speed within a segment from one time step to the next. This acceleration is only experienced by the vehicles that stay within the segment from one time step to the next. The temporal acceleration of the vehicles

[4] Based on statistical data one can also add a noise term to the average speed and average acceleration of the vehicles to capture the possible variation of the individual vehicles.

in the segment i of link m at time step k is thus given by

$$a_{m,i}^{\text{temp}}(k) = \frac{v_{m,i}(k+1) - v_{m,i}(k)}{T_{\text{s}}} \tag{16}$$

where the term 'temp' is a shorthand representation of 'temporal'.

Now let us determine the number of vehicles that are subject to this temporal acceleration from time step k to $k+1$. At time step k the number of vehicles in segment i is equal to $L_m \lambda_m \rho_{m,i}(k)$ and from time step k to $k+1$ the number of vehicles leaving segment i is $T_{\text{s}} q_{m,i}(k)$ (see Fig. A.2). Hence,

$$n_{m,i}^{\text{temp}}(k) = L_m \lambda_m \rho_{m,i}(k) - T_{\text{s}} q_{m,i}(k) \tag{17}$$

is the number of vehicles that stayed in segment i and that are subject to the temporal acceleration given in (16).

3.2. Spatial-Temporal Acceleration

The spatial-temporal acceleration is the change in speed experienced by vehicles moving from one segment of a link to another segment of the same link or of a different link. Depending on the geometry of the traffic network, there are several possible cases/scenarios for vehicles moving from one segment to another. In particular, the spatial-temporal acceleration from one segment to another segment is different for vehicles in a link and for vehicles crossing a node (an on-ramp, an off-ramp, merging links, and splitting links). In the sequel we discuss the spatial-temporal acceleration for each case.

3.2.1. Vehicles moving between consecutive segments within the same link

At the time step k the space-mean speed of the vehicles in segment i of link m is $v_{m,i}(k)$. In the next time step $k+1$ and in the next segment $i+1$, the speed will be $v_{m,i+1}(k+1)$. Thus, for time step k the spatial-temporal acceleration of the vehicles leaving segment i to segment $i+1$ of a link m is

$$a_{m,i,i+1}^{\text{spat}}(k) = \frac{v_{m,i+1}(k+1) - v_{m,i}(k)}{T_{\text{s}}} \tag{18}$$

where the term 'spat' is a shorthand representation of 'spatial-temporal'.

The number of vehicles that are subject to the spatial-temporal acceleration in (18) is obtained as

$$n_{m,i,i+1}^{\text{spat}}(k) = T_{\text{s}} q_{m,i}(k). \tag{19}$$

3.2.2. Vehicles crossing a node

General case

Let us consider the general case, where several incoming and outgoing links are connected to a node n as in Fig. A.3. In the figure, there are n_1 merging links

and n_2 splitting links. The spatial-temporal acceleration of vehicles moving from ingoing link m_i to outgoing link μ_j is given by

$$a^{\text{spat}}_{m_i,\mu_j}(k) = \frac{v_{1,\mu_j}(k+1) - v_{m_i,N_{m_i}}(k)}{T_{\text{s}}} \tag{20}$$

The corresponding number of vehicles subject to the spatial-temporal acceleration in (20) is given by

$$n^{\text{spat}}_{m_i,\mu_j}(k) = T_{\text{s}}\beta_{m_i,\mu_j}(k)q_{m_i,N_{m_i}}(k) \tag{21}$$

where $\beta_{m_i,\mu_j}(k)$ is the splitting rate of the flow from link m_i to the link μ_j.

Specific cases

- *On-ramp:* In METANET the speed of an on-ramp is not used. But, to determine the spatial-temporal acceleration of the vehicles moving from the on-ramp to the freeway, we need to assign the speed of the on-ramp. The speed is assumed to be based on measured or historic data in case no on-line measurements are available. Hence, we use the on-ramp speed $v_{\text{on},o}(k)$. In particular, for a situation like the one sketched in Fig. 4(a), the spatial-temporal acceleration and the number of vehicles subject to the acceleration are respectively

$$a^{\text{spat}}_{\text{on},o}(k) = \frac{v_{m,1}(k+1) - v_{\text{on},o}(k)}{T_{\text{s}}} \tag{22}$$

$$n^{\text{spat}}_{\text{on},o}(k) = T_{\text{s}}q_{\text{on},o}(k). \tag{23}$$

where $q_{\text{on},o}(k)$ is the on-ramp flow given by the equations of the form (6) or (7).

- *Off-ramp:* In general, the vehicles in the freeway can leave to the off-ramp o with an off-ramp speed $v_{\text{off},o}(k)$, where $v_{\text{off},o}(k)$ can be determined in a similar way as $v_{\text{on},o}(k)$. In particular in Fig. 4(b), the flow of the vehicles from segment N_m of link m (the freeway) to the off-ramp is given by

$$q_{\text{off},o}(k) = \beta_{m,o}(k)q_{m,N_m}(k) \tag{24}$$

  where $\beta_{m,o}(k)$ is the turning rate (i.e., the fraction of the flow of segment N_m of link m that flows to the off-ramp in the time period $[kT_{\text{s}}, (k+1)T_{\text{s}}]$).

  Now we can compute the spatial-temporal acceleration and the number of vehicles flowing from the segment N_m of link m to the off-ramp as

$$a^{\text{spat}}_{\text{off},o}(k) = \frac{v_{\text{off},o}(k+1) - v_{m,N_m}(k)}{T_{\text{s}}} \tag{25}$$

$$n^{\text{spat}}_{\text{off},o}(k) = T_{\text{s}}q_{\text{off},o}(k). \tag{26}$$

- *Lane drop/increase:* The spatial-temporal acceleration of vehicles moving from the last segment (with index N_m) of the first link m with λ_m lanes to the first segment of the second link $m+1$ with λ_{m+1} lanes is computed using the relation

$$a^{\text{spat}}_{m,m+1}(k) = \frac{v_{m+1,1}(k+1) - v_{m,N_m}(k)}{T_{\text{s}}}. \tag{27}$$

Moreover, the number of vehicles experiencing the acceleration is computed as

$$n^{\text{spat}}_{m,m+1}(k) = T_{\text{s}} q_{m,N_m}(k). \tag{28}$$

3.3. VT-macro

Unlike in the microscopic case where the speed-acceleration pair is for a single vehicle, the speed-acceleration pair generated in Sections 3.1 and 3.2 holds for a group of vehicles. Therefore, the emissions and fuel consumption obtained for the given speed-acceleration pair have to be multiplied by the corresponding number of vehicles in order to obtain the total emissions and fuel consumption. For example in Section 3.1 we have derived the temporal acceleration and the corresponding number of vehicles within a segment of a link at simulation step k. Using these variables as an input to the VT-micro model in (14), a new macroscopic emission and fuel consumption model for the vehicles moving within a segment is obtained as

$$\bar{J}^{\text{temp}}_{y,m,i}(k) = T_{\text{s}} n^{\text{temp}}_{m,i}(k) \exp\left(\tilde{v}_{m,i}(k) P_y \tilde{a}^{\text{temp}}_{m,i}(k)\right) \tag{29}$$

where $\bar{J}^{\text{temp}}_{y,m,i}(k)$ denotes the emission or fuel consumption $y \in \{\text{CO, HC, NO}_x, \text{CO}_2, \text{Fuel consumption}\}$ at simulation step k, the average acceleration vector $\tilde{a}^{\text{temp}}_{m,i}(k)$ and the average space-mean speed vector $\tilde{v}_{m,i}(k)$ are respectively obtained from $a^{\text{temp}}_{m,i}(k)$ and $v_{m,i}(k)$ by using the operator $\tilde{\cdot}$ defined in (14), while $a^{\text{temp}}_{m,i}(k)$ and $n^{\text{temp}}_{m,i}(k)$ are respectively given by (16) and (17), and $v_{m,i}(k)$ is the average space-mean speed of the vehicles in segment i of link m at simulation step k.

Similarly, using the corresponding speeds, accelerations, and number of vehicles, one can get the emissions or fuel consumption of vehicles moving from segment to segment within a link and vehicles crossing a node. Finally, the total emissions or fuel consumption of the vehicles in the traffic network at a simulation time step k is obtained by adding all together.

Thus, the interface block and the VT-micro block in Fig. A.1 forms a new macroscopic emission and fuel consumption model. We call this new model the "VT-macro" emission and fuel consumption model.

4. Analysis of VT-macro

In the previous section we have proposed the integration of the macroscopic traffic flow model METANET with the microscopic emission and fuel consump-

tion model VT-micro, which resulted in a macroscopic emission and fuel consumption model VT-macro. Due to the approximation of the speed and acceleration of the individual vehicles by the average speed and the average acceleration over the number of vehicles, the model may introduce errors. Moreover, the motive of the development of the model is to gain computational speed while keeping the estimation error as small as possible. Therefore, we now analyze the maximum error that can be introduced by this model.

In this section we want to examine the effect of going from one individual vehicle (VT-micro) to a group of vehicles (VT-macro). In general, we also could consider $T_\mathrm{s} \neq T_\mathrm{m}$. However, this problem is mainly related to traffic flow models (e.g. METANET vs. car-following). Here the focus of the analysis is only on the VT-macro model. Since the METANET model is not directly based on microscopic modeling approaches, we will not delve into the analysis of the approximation errors induced by the METANET traffic flow model. Hence, we assume here that $T_\mathrm{s} = T_\mathrm{m}$.

Let the speed of an individual vehicle α and the average speed over a group of vehicles be respectively $v_\alpha(\ell)$ and $\bar{v}(\ell)$. If the relative deviation of the speed v of an individual vehicle α from the average speed is $\delta_{v,\alpha}(\ell)$, then the speed of an individual vehicle can be expressed as

$$v_\alpha(\ell) = \bar{v}(\ell)(1 + \delta_{v,\alpha}(\ell)). \tag{30}$$

Similarly, let the acceleration of vehicle α be

$$a_\alpha(\ell) = \bar{a}(\ell)(1 + \delta_{a,\alpha}(\ell)) \tag{31}$$

where $\delta_{a,\alpha}(\ell)$ is the relative deviation of the acceleration of vehicle α from the average acceleration $\bar{a}(\ell)$.

In Section 3.3, the speed and acceleration inputs are transformed into a vector through the operator $\tilde{\cdot}$ defined in (14). Using the approximation relation $(1+\delta)^n \approx (1 + n\delta)$ for small δ, and the $\tilde{\cdot}$ operation, we get

$$\tilde{v}_\alpha(\ell) = (I + E\delta_{v,\alpha}(\ell))\tilde{\bar{v}}(\ell), \quad \tilde{a}_\alpha(\ell) = (I + E\delta_{a,\alpha}(\ell))\tilde{\bar{a}}(\ell)$$

where $E = \mathrm{diag}(0, 1, 2, 3)$, $\tilde{\bar{v}}(\ell) = [1\ \bar{v}(\ell)\ \bar{v}^2(\ell)\ \bar{v}^3(\ell)]^\top$, and $\tilde{\bar{a}}(\ell) = [1\ \bar{a}(\ell)\ \bar{a}^2(\ell)\ \bar{a}^3(\ell)]^\top$.

Hence, the emission $J_{\alpha,y}(\ell)$ of vehicle α with the speed $v_\alpha(\ell)$ and the acceleration $a_\alpha(\ell)$ can be expressed in terms of the average speed $\bar{v}(\ell)$, average acceleration $\bar{a}(\ell)$, speed deviation $\delta_{v,\alpha}(\ell)$, and acceleration deviation $\delta_{a,\alpha}(\ell)$ as

$$\begin{aligned} J_{\alpha,y}(\ell) = \exp\big[&\tilde{\bar{v}}^\top(\ell)P_y\tilde{\bar{a}}(\ell) + \delta_{v,\alpha}(\ell)\tilde{\bar{v}}^\top(\ell)EP_y\tilde{\bar{a}}(\ell) \\ &+\delta_{a,\alpha}(\ell)\tilde{\bar{v}}^\top(\ell)P_yE\tilde{\bar{a}}(\ell) + \delta_{v,\alpha}(\ell)\delta_{a,\alpha}(\ell)\tilde{\bar{v}}^\top(\ell)EP_yE\tilde{\bar{a}}(\ell)\big] \end{aligned} \tag{32}$$

Using the Taylor series expansion and neglecting higher-order terms of the deviations $\delta_{v,\alpha}$ and $\delta_{a,\alpha}$, the emission of vehicle α in (32) can be approximated to

$$\begin{aligned} J_{\alpha,y}(\ell) \approx \exp(\tilde{\bar{v}}^\top(\ell)P_y\tilde{\bar{a}}(\ell))\big[1 &+ \delta_{v,\alpha}(\ell)\tilde{\bar{v}}^\top(\ell)EP_y\tilde{\bar{a}}(\ell) \\ &+ \delta_{a,\alpha}(\ell)\tilde{\bar{v}}^\top(\ell)P_yE\tilde{\bar{a}}(\ell)\big]. \end{aligned} \tag{33}$$

Therefore, the relative error of the estimation of emissions and fuel consumption of individual vehicles due to the averaging of the speed and the acceleration is

$$\epsilon_{\text{approx},\alpha,y}(\ell) \approx \delta_{v,\alpha}(\ell)\tilde{\tilde{v}}^{\top}(\ell)EP_y\tilde{\tilde{a}}(\ell) + \delta_{a,\alpha}(\ell)\tilde{\tilde{v}}^{\top}(\ell)P_yE\tilde{\tilde{a}}(\ell). \qquad (34)$$

The operating region of the VT-micro emission model is described in (Rakha and Ahn, 2004) to be from 0 km/h to 120 km/h for the speed and from 0 m/s^2 to 2.75 m/s^2 for the acceleration. The maximum value of the acceleration range decreases linearly to zero as the speed increases from 35 km/h to 120 km/h. We simulate the model in its operating region to determine the maximum bound of the error in (34) for several possible combinations of the acceleration and speed ranges.

Fig. A.5 presents the maximum values of the approximate relative error (34) for all the possible speed and acceleration combinations within the operating region of the model when the deviations of the speed and acceleration are within ±5%. The colorbars on the right side of the plots show the maximum values of the approximate relative errors introduced by the model for combinations of the deviations $\delta_{v,\alpha}$ and $\delta_{a,\alpha}$.

5. Empirical Verification of VT-macro

In this section we evaluate the macroscopic VT-macro emission model by comparing it with the microscopic VT-micro emission model (14). To do so, we calibrate the microscopic car-following "intelligent driver model" (Treiber et al., 2000) to a calibrated macroscopic traffic flow METANET model for a Dutch highway. In the sequel we provide the description of the freeway, its modeling, and the results of the simulation based on the calibrated models.

5.1. Freeway and Scenario Description

The freeway stretch that we consider for the analysis of the VT-macro model is a part of the Dutch A12 freeway going from the connection with the N11 at Bodegraven up to Harmelen, and is shown in Fig. A.6. The freeway has three lanes in each direction. The part that we consider is approximately 14 km and it has two on-ramps and three off-ramps. The stretch is equipped with double-loop detectors at a typical distance of 500 to 600 m, measuring the average speed and flow every minute.

The data of the freeway has been used to calibrate the METANET model in (Hegyi et al., 2008). We use the same parameters that have been obtained in the study (Hegyi et al., 2008) to calibrate a microscopic car-following intelligent driver model (IDM) (Treiber et al., 2000). The IDM model was selected because in (Treiber et al., 2000) it was shown that this model improves the deficiencies of the well-known microscopic models GHR (Gazis et al., 1961) and OVM (Bando et al., 1995). The calibrated IDM car-following model will subsequently be coupled with the microscopic VT-micro emission and fuel consumption model.

In order to compare the performance of the integrated macroscopic flow and emission model with the microscopic flow and emission models, we use

four different traffic demand scenarios. In this way we can also show to some extent the robustness of the modeling approach presented in this paper. To provide a glimpse of the nature of the demand profiles, we provide the calibrating demand $d_{3,\text{cal}}$ in Fig. A.7, where the other demand profiles are related to the calibrating demand profile as $d_1(k) = 0.8d_{3,\text{cal}}(k)$, $d_2(k) = 0.9d_{3,\text{cal}}(k)$, and $d_4(k) = 1.1d_{3,\text{cal}}(k)$. The two integrated models (microscopic and macroscopic approaches) are then simulated for the four scenarios and the corresponding emissions, fuel consumption, and CPU time are collected. The results of the simulation are presented and discussed in the following section.

Moreover, to compare the newly developed dynamic-macroscopic emission and fuel consumption model, VT-macro, with average-speed-based macroscopic emission and fuel consumption model, we consider the COPERT (Ntziachristos and Samaras, 2000) model. We first integrate the COPERT model to the METANET model and next we calibrate the COPERT model in such a way that the error between the emission and fuel consumption estimates of the COPERT model and that of the VT-micro model is minimal. For the calibration process we use the demand profile $d_{3,\text{cal}}$. Since, it is suggested that the accuracy of average-speed-based emission and fuel consumption models can be improved if the speeds are averaged at shorter time intervals (Boulter et al., 2002), we follow the same strategy. Finally, we simulate the COPERT model as integrated with the METANET model and the VT-micro model as integrated to the IDM model for the four demand profiles aforementioned.

For the macroscopic simulation case the simulation time step is set to be 10 s, while for the microscopic the simulation time step is set to be 1 s.

5.2. Validation and Discussion

Recall that the VT-micro emission model estimates the emissions of each vehicle at specific times (every 1 s) and places. Therefore, to compare the results of the VT-macro model and COPERT with the VT-micro model, we have aggregated the emission estimates of the VT-micro model (or individual vehicles) over the 10 s time period in order to determine the total emission in a specific segment of the freeway. These integrated emission values during each 10 s of the VT-micro model are compared with the corresponding emission estimates of the VT-macro and the COPERT models.

Fig. A.8 provides plots of the estimates of the CO, HC, and NO_x emissions, and fuel consumption (FC) of the freeway for the demand scenario $d_1(k) = 0.8d_{3,\text{cal}}(k)$ that are estimated using the VT-micro, VT-macro, and COPERT models. The figure shows the evolution of the emissions and fuel consumption during the simulation period of about 1 h. Fig. A.8 clearly shows a very good fit of the estimates of the VT-macro model to the estimates of the VT-micro model, whereas the estimates of the COPERT show bad fit. The corresponding relative error of the macroscopic approaches with respect to the VT-micro is also presented in Fig. A.9. The figure clearly indicates that the estimation error[5] of

[5]The error in Fig. A.9 is not only due to the error introduced by the VT-macro model as

the VT-macro model is small for the this particular scenario, while that of the COPERT model is large.

We also computed the average of the absolute-relative-estimation error of the emissions and fuel consumption over the whole simulation time and the whole freeway. The results are presented in Table A.1 and Table A.2. Table A.1 indicates that the maximum average-absolute-relative error of the VT-macro model for these particular simulations is not more than 9.5%. So, although the model has been calibrated for a different demand profile, for the demand profiles d_1, d_2, and d_4 the estimates of the macroscopic approach are not far from the estimates of the microscopic approach. From Table A.2, one sees that the error that is introduced by the COPERT is more than three times the error introduced by the VT-macro for most of the cases.

In addition to the improvement of the emission estimation that can be obtained when microscopic emission models are integrated with macroscopic traffic flow models, the second motivation for the integration of the microscopic emission model with macroscopic traffic flow model is the need for reduced simulation time. In this regard we also compared the simulation time for the four different scenarios. In Table A.1 we provide the CPU time of the VT-micro (microscopic) and VT-macro (macroscopic) simulations versus the scenarios. It can be seen that the CPU time of the VT-macro simulation is independent of the demand (or number of vehicles) in the traffic network and is almost constant for all the four scenarios. On the other hand, the CPU time required for the simulation of the VT-micro model increases as the demand increases. Moreover, the CPU time required for the simulation of the VT-micro model is very large relative to the CPU time required by the VT-macro model to simulate the same traffic scenario.

6. Conclusions and Future Work

In this paper we have presented a general framework that can be used to integrate macroscopic traffic flow models with microscopic emission and fuel consumption models. We made a distinction between temporal and spatial-temporal variables in order to capture the discrete temporal and spatial nature of macroscopic traffic flow models. We further demonstrated the approach using the METANET traffic flow model and VT-micro emission and fuel consumption model that resulted in the VT-macro model.

Moreover, we have presented an analysis of the maximum approximate error that can be introduced by the use of macroscopic variables to determine the emissions and fuel consumption of individual vehicles. Both the analytic and empirical results show that the errors introduced by using VT-macro are

given in (34) and the COPERT model. The error is introduced both due the mismatch between the METANET and IDM traffic flow models and due to the mismatch between the VT-micro and VT-macro and between VT-micro and COPERT emission and fuel consumption models. Therefore, it is not possible to relate the errors in Fig. A.9 and with the approximate error in (34) nor between VT-micro and COPERT.

small. A comparison of the errors of the VT-macro model to the established average-speed-based macroscopic model, COPERT, also shows that the VT-macro model provides better estimates of the emissions and fuel consumption than the COPERT for the cases considered. Furthermore, the simulation results indicate that the simulation time (CPU time) can be tremendously decreased if one uses the macroscopically integrated emission model (VT-macro), while this only introduces errors less than 10% over the whole estimation for the particular scenarios.

In our future work, we will use the integrated models in model-based traffic control approaches to reduce emissions and fuel consumption. We will further compare and assess the performance of the VT-macro model for other traffic scenarios and network layouts.

Appendix A. VT-micro/macro parameters

The values of the model parameter P_y for the emission variables $y \in \{\text{CO, HC, } \text{NO}_x\}$ and the fuel consumption ($y = \text{FC}$) are given by:

$$P_{\text{CO}} = 0.01 \begin{bmatrix} -1292.81 & 48.8324 & 32.8837 & -4.7675 \\ 23.2920 & 4.1656 & -3.2843 & 0 \\ -0.8503 & 0.3291 & 0.5700 & -0.0532 \\ 0.0163 & -0.0082 & -0.0118 & 0 \end{bmatrix}, \tag{A.1}$$

$$P_{\text{HC}} = 0.01 \begin{bmatrix} -1454.4 & 0 & 25.1563 & -0.3284 \\ 8.1857 & 10.9200 & -1.9423 & -1.2745 \\ -0.2260 & -0.3531 & 0.4356 & 0.1258 \\ 0.0069 & 0.0072 & -0.0080 & -0.0021 \end{bmatrix}, \tag{A.2}$$

$$P_{\text{NO}_\text{x}} = 0.01 \begin{bmatrix} -1488.32 & 83.4524 & 9.5433 & -3.3549 \\ 15.2306 & 16.6647 & 10.1565 & -3.7076 \\ -0.1830 & -0.4591 & -0.6836 & 0.0737 \\ 0.0020 & 0.0038 & 0.0091 & -0.0016 \end{bmatrix}, \tag{A.3}$$

and

$$P_{\text{FC}} = 0.01 \begin{bmatrix} -753.7 & 44.3809 & 17.1641 & -4.2024 \\ 9.7326 & 5.1753 & 0.2942 & -0.7068 \\ -0.3014 & -0.0742 & 0.0109 & 0.0116 \\ 0.0053 & 0.0006 & -0.0010 & -0.0006 \end{bmatrix}, \tag{A.4}$$

when the inputs of the emission and fuel consumption model are in SI-units and the outputs are in kg/s for emissions and l/s for fuel consumption.

Acknowledgments

Research supported by the Shell/TU Delft Sustainable Mobility program, the Transport Research Center Delft, the European COST Action TU0702, the European 7th Framework Network of Excellence "Highly-complex and networked

control systems (HYCON2)", and the BSIK project "Next Generation Infrastructures (NGI).". We would also like to thank prof. Papageorgiou for the fruitful discussion on the topic of this paper, and for suggesting to undertake the theoretical analysis now reported in Section 4.

References

Ahn, K., Rakha, H., May 2008. The effects of route choice decisions on vehicle energy consumption and emissions. Transportation Research Part D 13 (3), 151–167.

Ahn, K., Trani, A. A., Rakha, H., M. Van Aerde, Jan. 1999. Microscopic fuel consumption and emission models. In: Proceedings of the 78^{th} Annual Meeting of the Transportation Research Board. Washington DC, USA, CD-ROM.

An, F., Barth, M., Nobeck, J., Ross, M., 1997. Development of comprehensive modal emissions model operating under hot-stabilized conditions. In: Proceedings of the 76^{th} Annual Meeting of the Transportation Research Board. Washington DC, USA, pp. 52–62.

Bando, M., Hasebe, K., Nakayama, A., Shibata, A., Sugiyama, Y., Feb. 1995. Dynamical model of traffic congestion and numerical simulation. Physical Review E 51 (2), 1035–1042.

Barth, M., An, F., Younglove, T., Scora, G., Levine, C., Ross, M., Wenzel, T., 2000. Comprehensive modal emissions model-CMEM. Tech. rep., University of California, Riverside, California, USA, version 2.0.

Boulter, P. G., Barlow, T., McCrae, I. S., Latham, S., Elst, D., E. van der Burgwal, 2002. Road traffic characteristics, driving patterns and emission factors for congested situations. Tech. rep., TNO Automotive, Department Powertrains-Environmental Studies & Testing, Delft, The Netherlands, OSCAR Deliverable 5.2.

Brackstone, M., McDonald, M., 2000. Car-following: a historical review. Transportation Research Part F 2 (4), 181–196.

Chang, M. F., Herman, R., Aug. 1981. Trip time versus stop time and fuel consumption characteristics in cities. Transportation Science 15 (3), 183–209.

Chen, D., Zhang, J., Tang, S., Wang, J., Dec. 2004. Freeway traffic stream modeling based on principal curves and its analysis. IEEE Transactions on Intelligent Transportation Systems 5 (4), 246–258.

Daganzo, C. F., Aug. 1994. The cell transmission model: A dynamic representation of highway traffic consistent with the hydrodynamic. Transportation Research Part B 28 (4), 269–287.

Daganzo, C. F., Apr. 1995. The cell transmission model, Part II: Network traffic. Transportation Research Part B 29 (2), 79–93.

Evans, L., Herman, R., 1978. Automobile fuel economy on fixed urban driving schedules. Transportation Science Information 12 (2), 137–152.

Gazis, D., Herman, R., Rothery, R., 1961. Nonlinear follow the leader models of traffic flow. Operations Research 9 (4), 545–567.

Hegyi, A., Hoogendoorn, S. P., Schreuder, M., Stoelhorst, H., Viti, F., Oct. 2008. SPECIALIST: A dynamic speed limit control algorithm based on shock wave theory. In: Proceedings of the 11^{th} International IEEE Conference on Intelligent Transportation Systems. Beijing, China, pp. 827–832.

Hoogendoorn, S. P., Bovy, P. H. L., Feb. 2000. Continuum modeling of multiclass traffic flow. Transportation Research Part B 34 (2), 123–146.

Hoogendoorn, S. P., Bovy, P. H. L., 2001. State-of-the-art of vehicular traffic flow modelling. Proceedings of the Institution of Mechanical Engineers, Part I: Journal of Systems and Control Engineering 215 (4), 283–303.

Huang, Z., Ma, X. X., Oct. 2009. Integration of emission and fuel consumption computing with traffic simulation using a distributed framework. In: Proceedings of the 12^{th} International IEEE Conference on Intelligent Transportation Systems. St. Louis, Missouri, USA, pp. 154–159.

Joumard, R., Jost, P., Hickman, J., Hassel, D., Jul. 1995. Hot passenger car emissions modelling as a function of instantaneous speed and acceleration. Science of the Total Environment 169 (1-3), 167–174.

Messmer, A., Papageorgiou, M., 1990. METANET: A macroscopic simulation program for motorway networks. Traffic Engineering and Control 31 (9), 466–470.

Ntziachristos, L., Samaras, Z., 2000. COPERT III. Computer program to calculate emissions from road transport. Methodology and emission factors. Tech. Rep. 49, European Environment Agency, Copenhagen, Denmark.

Oliver-Hoyo, M. T., Pinto, G., Feb. 2008. Using the relationship between vehicle fuel consumption and CO_2 emissions to illustrate chemical principles. Journal of Chemical Education 85 (2), 218–220.

Panis, L. I., Broekx, S., Liu, R., Dec. 2006. Modelling instantaneous traffic emission and the influence of traffic speed limits. Science of The Total Environment 371 (1-3), 270–285.

Pipes, L. A., Mar. 1953. An operational analysis of traffic dynamics. Journal of Applied Physics 24 (3), 274–281.

Qi, Y. G., Teng, H. H., Yu, L., Jun. 2004. Microscale emission models incorporating acceleration and deceleration. Journal of Transport Engineering 130 (3), 348–359.

Rakha, H., Ahn, K., Mar. 2004. Integration modeling framework for estimating mobile source emissions. Journal of Transport Engineering 130 (2), 183–193.

Treiber, M., Hennecke, A., Helbing, D., Aug. 2000. Congested traffic states in empirical observations and microscopic simulations. Physical Review E 62 (2), 1805–1824.

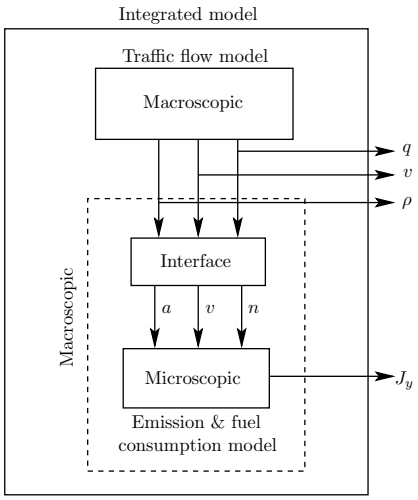

Figure A.1: Model integration block diagram. The output variables of the macroscopic traffic model are the average flow q, the average density ρ, and the average space-mean speed v. These variables are fed to the interface block. The interface block generates the acceleration a, the speed v, and the number of vehicles n that are inputs to the microscopic emission and fuel consumption model. Then, the macroscopic emission and fuel consumption model yields the emissions and the fuel consumption J_y of the traffic flow.

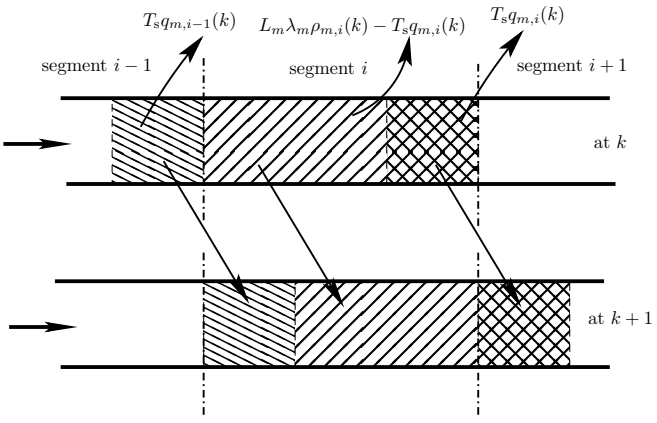

Figure A.2: Illustration of temporal and spatial traffic flow in METANET.

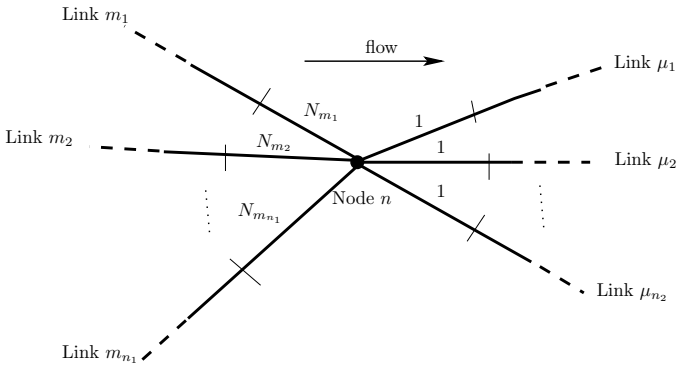

Figure A.3: General interconnection of road links at a node n.

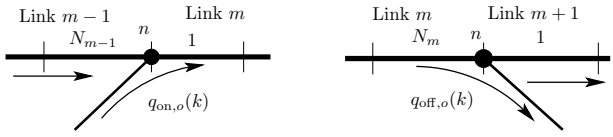

(a) on-ramp (b) off-ramp

Figure A.4: On-ramp and off-ramp.

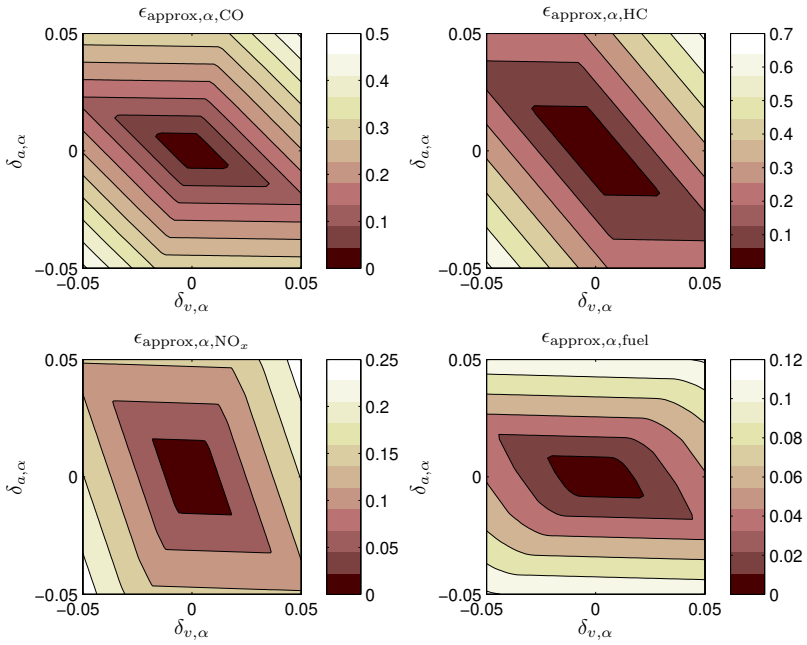

Figure A.5: Maximum values of the approximate error of (34) for different deviations of the speed $\delta_{v,\alpha}$ and acceleration $\delta_{a,\alpha}$ of an individual vehicle α for scenarios with average speeds (5–120km/h) and average accelerations (-5–2.75 m/s^2) respectively.

Figure A.6: A part of the Dutch A12 highway considered for the empirical verification of the VT-macro emission and fuel consumption model.

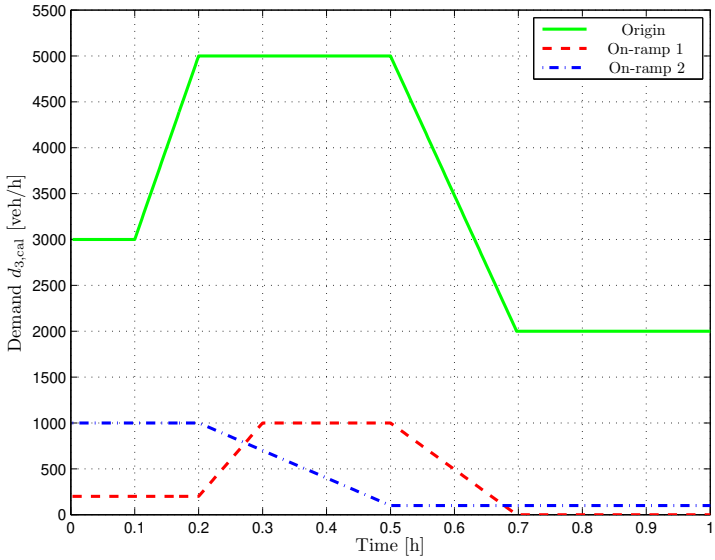

Figure A.7: Traffic demands scenarios used for the calibrating of the IDM model to the METANET model.

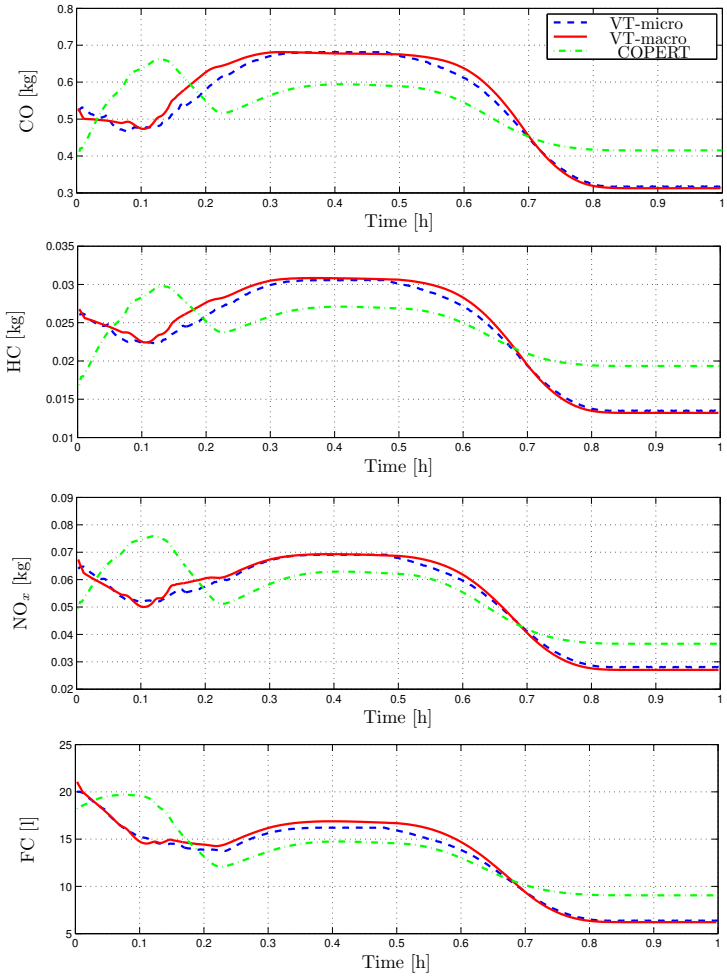

Figure A.8: Comparison of the emissions estimated using the macroscopic VT-macro and COPERT and the microscopic VT-micro emission and fuel consumption models for the demand profile $d_1(k) = 0.8 d_{3,\mathrm{cal}}(k)$.

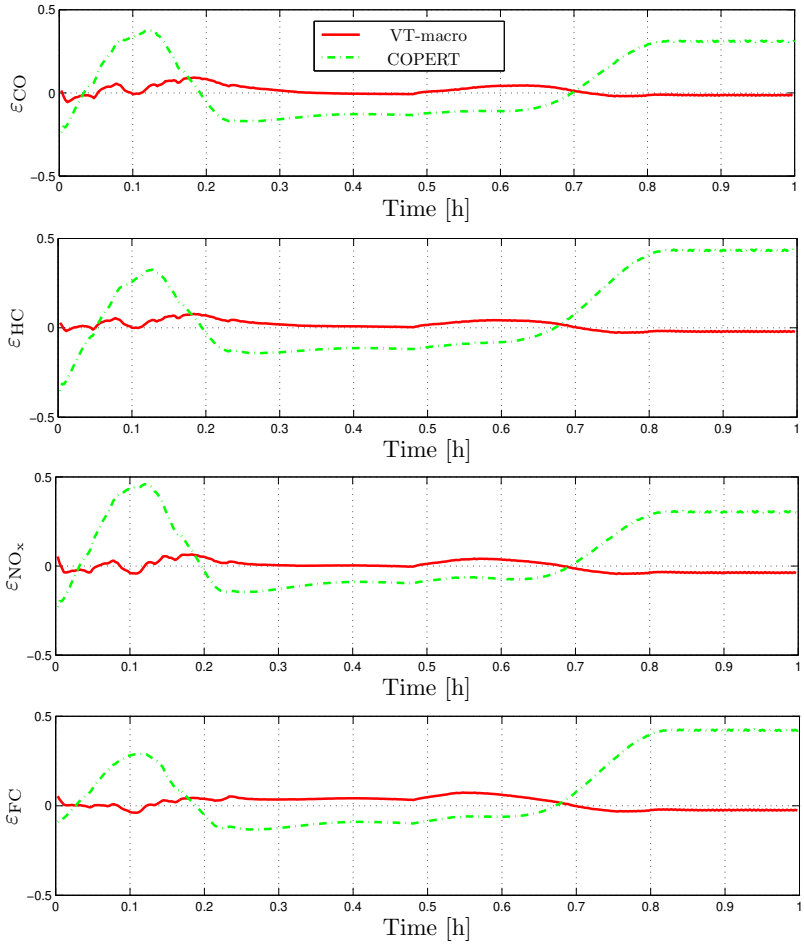

Figure A.9: Relative estimation error of the macroscopic VT-macro and COPERT models with respect to microscopic VT-micro model for the demand scenario $d_1(k) = 0.8 d_{3,\mathrm{cal}}(k)$.

Table A.1: The average of the absolute-relative error of VT-macro with respect to the VT-micro. The demand profiles are related as $d_1(k) = 0.8d_{3,\text{cal}}(k)$, $d_2(k) = 0.9d_{3,\text{cal}}(k)$, and $d_4(k) = 1.1d_{3,\text{cal}}(k)$.

Scenarios	Average-absolute-relative error (%)				CPU time (s)	
	CO	HC	NO_x	FC	VT-micro	VT-macro
d_1	2.4	2.5	2.5	3.2	112	1.70
d_2	2.3	1.9	2.7	2.6	124	1.52
$d_{3,\text{cal}}$	3.4	2.9	4.5	3.7	142	1.65
d_4	9.4	7.0	9.2	6.6	162	1.61

Table A.2: The average of absolute-relative error of COPERT with respect to the VT-micro. The demand profiles are related as $d_1(k) = 0.8d_{3,\text{cal}}(k)$, $d_2(k) = 0.9d_{3,\text{cal}}(k)$, and $d_4(k) = 1.1d_{3,\text{cal}}(k)$.

Scenarios	Average-absolute-relative error (%)			
	CO	HC	NO_x	FC
d_1	17.9	20.0	17.1	18.2
d_2	12.0	14.2	11.8	13.2
$d_{3,\text{cal}}$	6.7	9.3	7.9	9.0
d_4	7.5	10.0	8.0	7.0